Journal of Zhejiang University SCIENCE
ISSN 1009-3095
http://www.zju.edu.cn/jzus
E-mail: jzus@zju.edu.cn

The critical loading for lateral buckling of continuous welded rail

SUNG Wen-pei[†1], SHIH Ming-hsiang[2], LIN Cheng-I[3], GO Cheer Germ[4]

([1]*Department of Landscape Design and Management, National Chin-Yi Institute of Technology, Taiwan 41111, China*)

([2]*Department of Construction Engineering, National Kaoshiang First University of Science and Technology, Taiwan 824, China*)

([3]*Department of Fire Science, Wu-Feng Institute of Technology, Ming-Hsiung, Chiayi, Taiwan 621, China*)

([4]*Department of Civil Engineering, National Chung Hsing University, Taiwan 40227, China*)

[†]E-mail: sung809@chinyi.ncit.edu.tw

Received Jan. 30, 2005; revision accepted May 11, 2005

Abstract: The most significant differences between continuous welded rails (CWRs) and general split-type connectors are axial compression in the longitudinal direction, buckling stability and other issues generated under the influence of thermal effect. Under thermal effect, a dynamical behavior similar to that of a beam fixed on two sides occurs in the central locked area of the welded rail, as there is axial compression but no possibility of sliding. Continuous welded rails do not contract or expand, and are supported by the dynamical system made up of ballasts and rail clips. The rail-support system mentioned above has the features of non-uniform material distribution and uncertainty of construction quality. Due to these facts, the dynamics method based on the linear elastic hypothesis cannot correctly evaluate the rail's buckling conditions. This study is aimed at applying Finite Difference Method (FDM) and Monte Carlo Random Normal Variables Method to the analysis of welded rail's buckling behavior during the train's acceleration and deceleration, under thermal effect and uncertain factors of ballast and rail clips. The analysis result showed that buckling occurs under the combined effect of thermal effect and the train's deceleration force co-effect and the variance ratio of ballast and rail clips is over 0.85, or under the combined effect of thermal effect and the train's acceleration force when the variance ratio is over 0.88.

Key words: Thermal effect, Finite Difference Method, Monte Carlo Method, Buckling load
doi:10.1631/jzus.2005.A0878 **Document code:** A **CLC number:** TU375

INTRODUCTION

The conventional design of rails uses steel clip boards and bolts to link rails, and avoids buckling caused by thermal expansion effect by mounting expansion joints to solve axial restraint generated by seasonal or day-and-night temperature changes. But the discontinuity at the rail joints brings discomfort and noise to passengers when the train has suddenly stops or starts, during which train speed cannot be effectively increased, rails are more easily damaged, and the cost of maintenances of trains and rails is relatively higher. There was a tendency of replacing expansion joints with continuous joints in resolving these problems by increasing the length of seamless rails. Welding is a suitable method currently used in Taiwan's mass and rapid transit systems and the high-speed railway system. Besides, Japan even further improved it and applied it to turnouts and sharp curves (Miura and Yanagawa, 1992). Due to the drastic change of temperature in Taiwan and the reduced use of expansion joints, problems such as longitudinal axial compression and buckling are likely to occur under the impact of thermal effect. That is to say, on a CWR (continuous welded rail) that is tens meters long, despite the mounting of expansion joints on the two ends, dynamical behavior similar to that of

[*] Project supported by the National Science Council of Taiwan (No. NSC 93-2211-E-167-002), China

beam fixed on two sides will occur at the central area (locked area) of the rail. The CWR cannot slip to move slide longitudinal coordinate, as a result the CWR must bear the tremendous axial compression force. If the temperature soars to high and CWR has insufficient support of lateral force, lateral buckling of rail easily occurs when the train rumbles by.

In the analysis of rail buckling, Kerr (1973; 1974a; 1974b; 1969; 1975; 1978) and Kawaguchi (1969; 1971) categorized the buckled rails they observed and studied into two kinds: those with buckling occurring in vertical direction; and those with buckling occurring at the horizontal side. Although the transformation model of rail buckling can be three-dimension, the above hypotheses are intended to simplify the analysis. Kerr (1973; 1974a; 1974b; 1969; 1975; 1978) divided his study into two parts: one in which the rail is supposed to be a flexible beam mounted to elastic foundation; and the other in which the rail is supposed to be a beam mounted to a fixed base subjected to uniformly distributed load, and when a part of the rail is upheld off the base, buckling load condition will be reached. But after comparison of theories and empirical buckling models, it was discovered that the rail is in contact with the base both before and after the buckling; therefore, this analysis model is not suitable for analyzing vertical buckling. Kerr (1978) derived a non-linear governing equation of rail expansion resulted from thermal effect by using virtual displacement method. It can be derived from this equation that the highest safe temperature is the lowest rising temperature, which infers that when the temperature is over the lowest rising temperature, the rail will be upheld and deformed. So the equation of lowest rising temperature is the equilibrium equation of upholding deformation. Kawaguchi (1969; 1971) used relevant theories and experimental methods for studying the buckling problem of ground cement board caused by its thermal expansion. This kind of problem is very close to the problem of the rail stability when axial force is greater than the bottom value of buckling load; the system is in two states of balance: one is the balance before buckling occurs, and the other is the balance as the result of a stable state of CWR that occurs after CWR produces great deformation. Whether it be Kerr's lowest rising temperature or Kawaguchi's bottom value of buckling load, both are two necessary conditions of buckling balance; the values are conservative estimates of buckling load.

Taiwan High-speed Railway, currently under construction, also adopts continuous welded rails (CWRs) in its construction. Under the effects of temperature changes and the train's stops and starts, CWR differs greatly from the conventional bolt joint system in terms of transferred longitudinal force and size of this force. CWR cannot expand freely in long direction, but CWR buttons up the piece to become ballast and rail clips of common mechanical system delivering the induced force: on one hand, when the thermally induced contraction and expansion generate iterative action between ballast/clips and the rails, causes axial deformation under the axial force effects; and on the other hand, carries the train's longitudinal load. The ballast and rail clips mainly supply stiffness to resist the vertical and lateral deformation induced by axial force. The mechanical behavior of ballast and rail clips can be treated as elastic behavior of the foundation. The deformation behavior of CWR is affected by the vertical and lateral deformation, influenced by ballast and rail clips. Thus, this study applies energy method to derive the system's critical load of lateral resistance that CWR can endure. In order to analyze the iterative action between ballast/clips and rails, the Finite Difference Method is proposed to derive the critical load of CWR and apply Monte Carlo Random Variables Method for simulating lateral resistance force that ballast and clips can provide.

ANALYSIS MODEL

According to field observation (Huang, 2001), when a continuous welded rail is subjected to axial compression, CWR deformation occurs vertically when ballast and rail clips become invalid, buckling usually occurs in the lateral direction. As Fig.1 shows, the moment force at the inflection point is zero. Thus, we take the length between the two neighboring points and analyze the lateral buckling of the rail. As the moment force at the inflection point is zero, this inflection point can be simulated as hinge links.

Buckling length of minimum critical load

Both ends of the beam-column system placed on

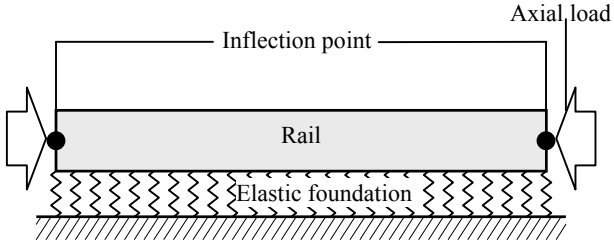

Fig.1 A sketch map for lateral resistance force, supplied by ballasts and rail clips

an elastic foundation, are hinge connections. The energy method can be applied to derive its buckling load.

Firstly, assume the bucking curve is $y=\sum_{n=1}^{\infty} a_n \sin\frac{n\pi x}{l}$, where l is the distance between two adjacent inflection points. Therefore, systematic bending strain energy V_b is:

$$V_b=\frac{EI}{2}\int_0^l\left(\frac{d^2y}{dx^2}\right)dx=\frac{\pi^4 EI}{4l^3}\sum_{n=1}^{\infty}n^4a_n^2 \tag{1}$$

The unit lateral resistance force, supplied to the rail by the ballast and rail clip, is shown in Fig.2. The formula is expressed as follows:

$$\beta(x)=\begin{cases}\left[1-\frac{H}{2d}\left(1+\sin\frac{\pi x}{l}\right)\right]^2 k_o, & 1\geq H/d\geq 0\\ 0, & H/d>1\end{cases} \tag{2}$$

where k_o is the unit lateral resistance force of ballast and rail clips to the rail before it is lifted; d is the depth of rail clip covered into the sleeper and ballast; H is the lift height.

Then, the total energy V_f induced by the deformation of the rail in the vertical direction when the ballast and rail clips lose efficiency is as Eq.(3):

$$V_f=\int_0^l\frac{\beta(x)}{2}y^2dx \tag{3}$$

Substituting Eq.(2) into Eq.(3) yields,

$$V_f=\frac{a_n^2k_o}{2}\left[\left(1-\frac{H}{d}\right)\int_0^l\left(\sin^2\frac{n\pi x}{l}dx\right)-\frac{H}{d}\int_0^l\left(\sin^2\frac{n\pi x}{l}\sin\frac{\pi x}{l}\right)dx+\left(\frac{H}{2d}\right)^2\int_0^l\left(1+\sin\frac{\pi x}{l}\right)^2\sin^2\frac{n\pi x}{l}dx\right] \tag{4}$$

According to the minimum potential energy principle, the n is assigned to 1, thus $y=a_1\sin(x/l)$. Therefore, Eq.(4) can be rearranged as Eq.(5):

$$V_f=\frac{a_1^2k_o}{2}\left[\frac{l}{2}-\left(\frac{l}{2}+\frac{4l}{3\pi}\right)\frac{H}{d}+\left(\frac{7l}{8}+\frac{8l}{3\pi}\right)\frac{H^2}{4d^2}\right] \tag{5}$$

The work done by the axial pressure p is:

$$V_p=p\frac{1}{2}\int_0^l\left(\frac{dy}{dx}\right)^2dx=\frac{p\pi^2}{4l}a_1^2 \tag{6}$$

According to the virtual work principle, therefore

$$\Delta V=\delta^2V/2\cong V_b+V_f-V_p.$$

Then, the critical load can be acquired as:

$$P_{cr}=\frac{\pi^2EI}{l^2}+\frac{k_ol^2}{\pi^2}\left[1-\left(1+\frac{8}{3\pi}\right)\frac{H}{d}+\left(\frac{7}{16}+\frac{4}{3\pi}\right)\frac{H^2}{d^2}\right] \tag{7}$$

At this time, critical load is expressed by an equation regarding system length l as the variable of the equation. So, the minimum critical load can be derived from the first order derivative Eq.(7) to obtain the system length of the steel rail, as Eq.(8):

$$l=\pi\sqrt[4]{\frac{EI}{\left[1-\left(1+\frac{8}{3\pi}\right)\frac{H}{d}+\left(\frac{7}{16}+\frac{4}{3\pi}\right)\frac{H^2}{d^2}\right]k_o}} \tag{8}$$

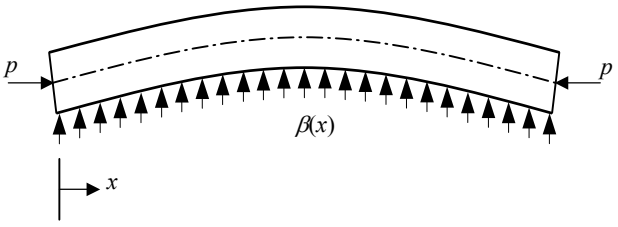

Fig.2 A sketch map for unit lateral resistance force, supplied by ballasts and rail clips to rail

Substitution of Eq.(8) into Eq.(7) yields the critical load of the rail as Eq.(9):

$$P_{\mathrm{cr}}=2\sqrt{EIk_{\mathrm{o}}\left[1-\left(1+\frac{8}{3\pi}\right)\frac{H}{d}+\left(\frac{7}{16}+\frac{4}{3\pi}\right)\frac{H^2}{d^2}\right]} \quad (9)$$

where H/d is limited to $1\geq H/d\geq 0$; E is elastic modulus of rail; I is rail's area moment of inertia.

If $H/d>1$ is obtained, then $V_{\mathrm{b}}=\dfrac{\pi^4 EI}{4l^3}\sum_{n=1}^{\infty}n^4a_n^2$, $V_{\mathrm{f}}=0$, $V_{\mathrm{p}}=\dfrac{P\pi^2}{4l}\sum_{n=1}^{\infty}n^2a_n^2$. Again, according to the principle of virtual work and principle of minimum potential energy, the critical load can be expressed as follows:

$$P_{\mathrm{cr}}=\pi^2EI/l^2.$$

That is, when the lateral resistance force of the ballast is zero, the buckling load of rail becomes the buckling load of the rail itself.

Lateral resistance force of rail

According to elasticity theories (Pilkey, 1994) and small deformation theory, parameter of time can be ignored. Given that a continuous elastic beam system with well-dispersed materials, under a static load, with axial compression P and strength $q(x)$ distribution of lateral load, we can derive the formulation of its lateral deflection as follows:

$$EI\frac{\mathrm{d}^4y}{\mathrm{d}x^4}+P\frac{\mathrm{d}^2y}{\mathrm{d}x^2}=q(x)$$

The lateral resistance force of the rail is correlated to the ballasts depth, construction accuracy, material uniformity of the ballast and rail clips, and so on. The distributed lateral load can be presumed on the basis that the rail is mounted on elastic foundation of flexible springs; so, $q(x)=-\beta(x)y$ and the governing equation of lateral deflection can be expressed as Eq.(10):

$$EI\frac{\mathrm{d}^4y}{\mathrm{d}x^4}+P\frac{\mathrm{d}^2y}{\mathrm{d}x^2}=-\beta(x)y\,. \quad (10)$$

This is the governing equation of rail, discussed in this paper, subjected to non-uniform lateral resistance force. The elastic foundation stiffness $\beta(x)$, induced by ballast and rail clips shown in Eq.(2), is a function of location and center point displacement ($H=y(l/2)$). As a result, Eq.(10) is a fourth order nonlinear ordinary differential equation, and will be analyzed with Finite Difference Method in this research.

Finite Difference Method for analyzing lateral buckling of CWR

As lateral resistance force of CWR is mainly provided by ballast and joint clips, the commonly used energy method cannot correctly simulate lateral resistance force of CWR, so Finite Difference Method (FDM) was employed to simulate the lateral resistance force of CWR.

Firstly, CWR was used to equally divide the effective length into $(n-1)$ parts. And then the central difference at point i was substituted into Eq.(10) satisfying a local balance. Eq.(10) can be denoted as shown in Eq.(11):

$$\begin{aligned}&\frac{EI}{\Delta l^4}\begin{bmatrix}1 & -4 & 6 & 4 & 1\end{bmatrix}\begin{bmatrix}y_{i-2} & y_{i-1} & y_i & y_{i+1} & y_{i+2}\end{bmatrix}^{\mathrm{T}}\\&+\frac{P}{\Delta l^2}\begin{bmatrix}0 & 1 & -2 & 1 & 0\end{bmatrix}\begin{bmatrix}y_{i-2} & y_{i-1} & y_i & y_{i+1} & y_{i+2}\end{bmatrix}^{\mathrm{T}}\\&=\bar{W}_i\end{aligned} \quad (11)$$

where

$\bar{W}_i=-\begin{bmatrix}0 & 0 & \beta_i & 0 & 0\end{bmatrix}\begin{bmatrix}y_{i-2} & y_{i-1} & y_i & y_{i+1} & y_{i+2}\end{bmatrix}^{\mathrm{T}}$;
l is shown in Eq.(8).

Combine the equilibrium equations from point 1 to n into the matrix form shown in Eq.(12):

$$\boldsymbol{A}\{y\}+P_{\mathrm{cr}}\boldsymbol{B}\{y\}=\boldsymbol{CD}\{y\} \quad (12)$$

where

$$\boldsymbol{A}=\frac{EI}{\Delta l^4}\begin{bmatrix}5 & -4 & 1 & 0 & & 0\\-4 & 6 & -4 & 1 & 0 & \\1 & & \ddots & & & \\0 & & & \ddots & & 1\\ & & & & 6 & -4\\0 & & & 1 & -4 & 5\end{bmatrix},$$

$$\boldsymbol{B}=\frac{1}{\Delta l^2}\begin{bmatrix} -2 & 1 & 0 & & & 0 \\ 1 & -2 & 1 & 0 & 0 & \\ 0 & & \ddots & & & \\ & & & \ddots & & 0 \\ & & & & \ddots & 1 \\ 0 & & & 0 & 1 & -2 \end{bmatrix},$$

$$\boldsymbol{C}=\begin{bmatrix} \beta_1 & 0 & & & & 0 \\ 0 & \beta_2 & 0 & & & \\ & 0 & \ddots & 0 & & \\ & & 0 & \ddots & 0 & \\ & & & 0 & \ddots & 0 \\ 0 & & & & 0 & \beta_n \end{bmatrix}.$$

$\boldsymbol{A}$ represents the matrix of the finite difference fourth order term. The two ends are hinge links, so the first and the last element on the diagonal term should be 5; $\boldsymbol{B}$ is the matrix of the finite difference second order term; $\boldsymbol{C}$ is the matrix composed of various base moduli and different lateral resistance; $\boldsymbol{D}$ is the quadratic distributed concentrated load

Eq.(12) yields,

$$P\{y\}=\{\boldsymbol{CD}-\boldsymbol{A}\}\boldsymbol{B}^{-1}\{y\}. \tag{13}$$

Eq.(13) can be rewritten as the following characteristic Eq.(14):

$$\lambda\{y\}=\boldsymbol{H}\{y\} \tag{14}$$

Solution of the eigenvalue Eq.(14) yields the eigenvalue λ, which is the critical load of rail's lateral buckling.

$$\lambda=P_{\mathrm{c}}. \tag{15}$$

Simulation of the non-uniform lateral resistance force characteristic with Monte Carlo Method

The lateral resistance provided by ballast and that provided by rail clips while they are becoming ineffective has the characteristic of non-uniform distribution. The lateral resistance β from ballast and rail clips, and its maximum possible derivation value $\Delta\beta/\beta$ were used in the numerical experiment. The random values generated using the binary code can be expressed as Eqs.(16) and (17):

$$X_{n+1}=(aX_n)-\mathrm{int}[(aX_n)/M]\cdot M \tag{16}$$

$$RAN=2X_{n+1}/M-1 \tag{17}$$

where X_n is the remainder of nth order sampling; X_{n+1} is the remainder of $(n+1)$th order sampling; a is randomly selected natural number; M is 2^b-1 and b is a natural number; RAN is the random number between 1 and -1.

The systems of the ballast and rail clip have some hardly controllable problems causing the exact truth to deviate from actual expectation. Consideration of the different conditions of each possible situation caused by the system variation can be done by the random variable selection to simulate the CWR lateral resistance force on condition that:

(1) The random variable is normal distribution mode;

(2) The distribution situation is 99.7% of weight factor plus/minus 100%;

(3) The standard deviation is 1/3.

The normal random variable can be obtained through the uniform distribution random variation on central limit theorem. From Eq.(16), let

$$RAN_{\mathrm{u}}=X_{n+1}/M \tag{18}$$

RAN_{u} is the uniform random variable between 0 and 1. The normal random variable RAN_{n} (Naylor, 1966) can be obtained with Eq.(19):

$$RAN_{\mathrm{n}}=\frac{\sigma}{\sqrt{n/12}}\sum_{i=1}^{n}(RAN_{\mathrm{u}})_i+\left(\mu-\frac{n}{2}\frac{\sigma}{\sqrt{n/12}}\right) \tag{19}$$

where n is the number of homogeneous distribution random variables; μ is the mean value of normal distribution; σ is the standard deviation of normal distribution.

The random values derived from Eqs.(16)~(19), the lateral resistance β_i from ballast and rail clips on random location of elastic foundation can be simulated as shown in Eq.(20):

$$\beta_i=\beta\left[\left(1-\frac{\Delta\beta}{\beta}\right)+\left(\frac{\Delta\beta}{\beta}RAN_{\mathrm{n}}\right)\right] \tag{20}$$

This equation is only valid when $0\le H/d\le 1$; and if $H/d>1$, lateral resistance should be changed as $\beta_i=0$.

Putting Eq.(20) into Eqs.(10)~(15), yields the critical lateral buckling load P_{cr} of rail.

Influence of thermal effect, acceleration and deceleration forces

Because of Taiwan's geographical location, with high temperature and humidity in summer and great temperature difference under radiation cooling effect in winter, the impact of thermal effect cannot be neglected. In addition to lateral force of rail, acceleration and deceleration forces of the train can also result in buckling. So, this study is focused on the influence of thermal effect, acceleration and deceleration forces.

The influence of thermal effect on rail's axis compression can be calculated with the use of Eq.(21).

$$P = \alpha \Delta T A E \tag{21}$$

where P is axis compression of rail increased by thermal effect; α is heat expansion factor of rail (Given as 1.18×10^{-5} °C); ΔT is temperature difference; A is cross-sectional area of rail; E is elastic modulus of rail.

Acceleration and deceleration forces were determined [in accordance with the German specification and the European standard, Eurocode 1 (1994)] to evaluate the impact of acceleration force of 1000 kN distributed equally within 30 m, and deceleration force of 20 kN/m.

NUMERICAL ANALYSIS RESULTS

During numerical analysis, refer to the following given conditions were referred to for verifying the critical lateral buckling load of rail:

(1) The full cross section of rail is homogeneous and isotropic;

(2) The rail lateral resistance force is provided by ballast and rail clips on two sides of rail is not uniformly distributed type, and size of the force is co-related to the rail's transformation;

(3) The rail deforms in weak axis directions.

The CWR model adopted in this analysis was 50 kg/m. Its material properties are: Young's modules E: 2.06×10^4 kN/cm^2; Poisson ratio υ: 0.27; Shear modulus G: 7.50×10^4 kN/cm^2; Thermal expansion coefficient α: 1.18×10^{-5} °C; Cross section of CWR: 64.20 cm^2; Base width of CWR: 12.5 cm; Height of CWR: 15.30 cm; Moment of inertia of strong axis: 1968 cm^4; Moment of inertia of weak axis: 301.68 cm^4. According to the design specification (Eurocode 1, 1994), each rail clip and ballast is designed to provide lateral resistance force of 8 kN/m, and the lateral resistance distributed on the rail is determined by normal random variables.

This analysis model primarily focused on the non-uniform lateral resistance phenomenon resulted from non-uniform depths of ballasts buried in the base due to rail deformation and erosion and abrasion of rail clips. In order to carry out an in-depth study on the influence of these factors, the rail is divided into 5 and 7 different cross sections. The maximum possible deviation values of rail lateral resistance force are taken as $\Delta\beta/\beta$=0.05, 0.1, 0.2, 0.5, 1.0 for numerical experiments on the above 5 various conditions with 1000 times numerical analysis in Monte Carlo Method. The results of critical load analysis of with different cross section are listed in Tables 1 and 2. The analysis results of two different sections are shown in Figs.3. And the relation of the critical load with different cross sections and $(\Delta\beta/\beta)_{max}$ is shown in Fig.4.

Table 1 The relationship of P_{cr} of partition 5 cross section and $\Delta\beta/\beta$

$\Delta\beta/\beta$	$(P_{cr})_{max}$ (kN)	$(P_{cr})_{avg}$ (kN)	$(P_{cr})_{min}$ (kN)
1.0	1892.67	1214.91	551.60
0.5	1954.69	1715.05	1524.87
0.2	1981.76	1899.50	1830.55
0.1	1987.58	1948.00	1912.23
0.05	1990.47	1971.02	1952.89

Table 2 The relationship of P_{cr} of partition 7 cross section and $\Delta\beta/\beta$

$\Delta\beta/\beta$	$(P_{cr})_{max}$ (kN)	$(P_{cr})_{avg}$ (kN)	$(P_{cr})_{min}$ (kN)
1.0	1687.90	1107.76	532.35
0.5	1794.14	1577.26	1351.65
0.2	1856.52	1772.77	1680.10
0.1	1979.97	1835.90	1788.93
0.05	1983.87	1867.25	1843.26

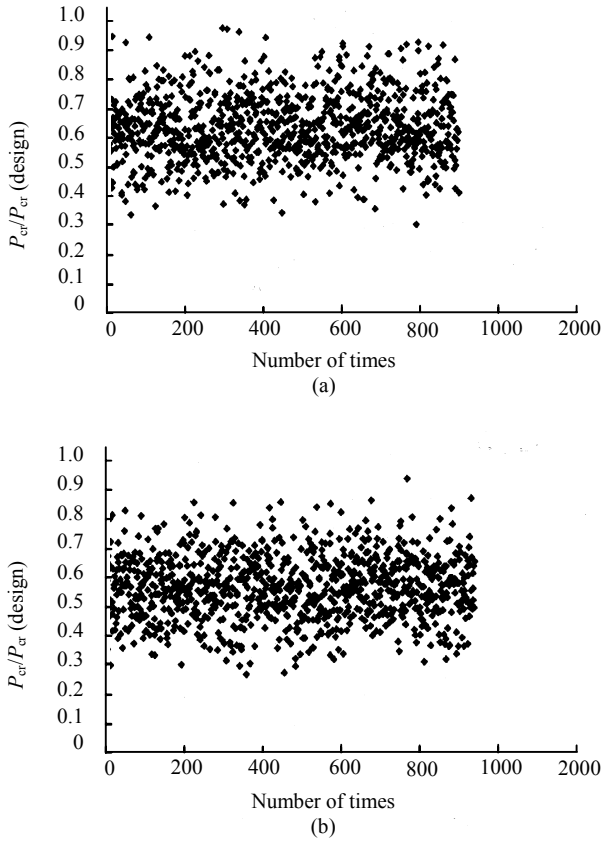

Fig.3 Monte Carlo to analyze with the random normal variable method 1000 times of data distribute for partition five kinds of cross section (a) and for partition seven kinds of cross section (b)

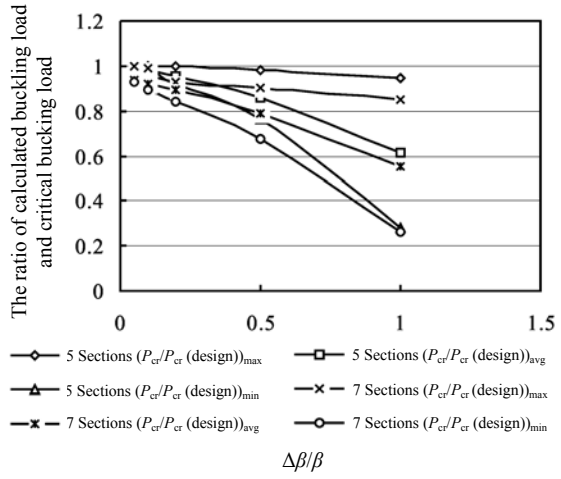

Fig.4 The relationship of critical load with various partition cross sections and $(\Delta\beta/\beta)_{max}$

DISCUSSION

The analysis result showed that when $(\Delta\beta/\beta)_{max}$=1.0, the minimum value of the rail's critical load is reduced to 557.16 kN, and its axial resistance ability decreases about 72%. When the temperature rises to 40 °C, and internal axial compression has reached 624.23 kN, rail buckling occurred. When combined actions of thermal effect and the train's deceleration force, and the ballast and rail clip's variance ratio $(\Delta\beta/\beta)_{max}$ is above 0.85; or when combined actions of thermal effect and the train's acceleration force, and the variance ratio $(\Delta\beta/\beta)_{max}$ is over 0.88, buckling phenomenon of rail will occur. This is because under these two conditions, the lateral resistance force provided by ballast and rail clips is not enough for resisting deceleration and acceleration forces and the increasing axial force increased under thermal effect. When the variance ratio $(\Delta\beta/\beta)_{max}$ reaches 1.0, the deducted value of the base modulus is around 0.74~0.79; that is to say, the lateral resistance ability is only 21%~26% of the designed buckling load. When the temperature rises to 20 °C, the axial compression ability of the rail is only 5.34%~10.34% of the pre-defined buckling load.

The investigation report (Huang, 2001) on the damage of Taiwan's Nankang River Bridge in a traffic accident of the TRA's south-bound train, Chu-Kuang No. 41 showed that the damage on the site was a first buckling model, with the buckling length 6 m long, and the critical loading 323.4 kN. Refer the critical load in Fig.4. The base deducted value was about 0.91~0.94; that is to say, at this point, the lateral resistance of the rail remained only 6%~9%. The rail temperature was detected to be 46 °C. Obviously, due to thermal effect, buckling occurred before the train arrived, mainly because the support of ballast and rail clips completely failed here at this time. Thus it can be inferred that the subsidence of ground base near that area was considerably serious.

CONCLUSION

According to the above numerical analysis, the greater the variance ratio of ballast and rail's clips, the smaller was the lateral resistance force provided by the rail. If thermal effect is considered, their ability to resist lateral force drops drastically. If acceleration and deceleration forces of the train are further considered, buckling is more likely to occur and even

lead to the derailment of the train.

Listed below are 3 suggestions for ensuring the safety of train transportation:

1. Carry out maintenance, repair, and inspection of ballasts and rail clips, and check and renew defective or old rail components;

2. In seasons with drastic temperature changes, check carefully the conditions of ballasts and rail clips, to ensure the safety of transportation;

3. Adopt construction methods that enhance lateral support stresses; for instance, adopt the stress-increasing rail protection method, and increase the rail's designed lateral resistance force.

References

Eurocode 1, 1994. Basis of Design and Actions on Structures Part 3: Traffic Loads on Bridges. CEN.

Hillier, F.S., Lieberman, G.J., 1974. Operation Research, 2nd Edition. Holdenday, Inc.

Huang, Y.L., 2001. Research on the Buckling and Fatigue Properties of Rail. Research report, Department of Civil Engineering, National Chung Hsing University, Taiwan.

Kawaguchi, M., 1969. Thermal buckling of continuous pavement. *Proceedings of the Japan Society of Civil Engineering*, **170**:331-334.

Kawaguchi, M., 1971. Snap-through buckling of blocks laid in a line. *Proceedings of JSED*, **193**:125-133.

Kerr, A.D., 1969. Buckling of continuously supported beams. *Journal of Engineering Mechanics Division*, *Proceedings of the ASCE*, **95**(2):247-253.

Kerr, A.D., 1973. A Model Study for Vertical Track Buckling. *High Speed Ground Transportation Journal*, **7**(3):351-368.

Kerr, A.D., 1974a. The stress and stability analyses of railroad tracks. *Journal of Applied Mechanics*, *Transactions of ASME*, p.841-848.

Kerr, A.D., 1974b. On the Stability of the Railroad Track in the Vertical Plane. Rail International, p.131-142.

Kerr, A.D., 1975. Lateral Buckling of Railroad Tracks Due to Constrained Thermal Expansions−A Critical Survey. Proceedings Symp. On Railroad Track Mechanics, Pergamon Press, p.141-169.

Kerr, A.D., 1978. Determination of admissible temperature increases to prevent vertical track buckling. *Journal of Applied Mechanics, Transactions of the ASME*, **45**(3):565-573.

Miura, S., Yanagawaa, H., 1992. Extended applicability of continuous welded rail. *Japanese Railway Engineering*, **120**:21-25.

Naylor, T.H., 1969. Computer Simulation Techniques. John Wiley and Sons.

Pilkey, W.D., 1994. Formula for Stress, Strain and Structural Matrices. John Wiley & Sons, Inc.